Development of monoblock TM dielectric resonator filters with additive manufacturing

Carlos Carceller[1], Fabrizio Gentili[1], Dominik Reichartzeder[2], Wolfgang Bösch[1], Martin Schwentenwein[2]

[1]Institute of Microwave and Photonic Engineering, Technische Universität Graz, Inffeldgasse 12, 8010 Graz, Austria. Email: carlos.carcellercandau@tugraz.at, fabrizio.gentili@tugraz.at
[2]Lithoz GmbH, Mollardgasse 85A, 1060 Vienna, Austria

Abstract: TM dielectric resonator filters are frequently affected by a poor contact in the interface between metal and ceramic walls, misalignment of the ceramic parts, and cracks due to mechanical stress. To overcome these issues, the present paper proposes the development of monoblock filters fabricated by lithography-based ceramic manufacturing. In order to build these structures with additive manufacturing, some geometrical changes, with respect to the classical assembly, have to be applied. The effect of these changes on the electrical performance of a stand-alone resonator are studied. Then, a filter prototype is manufactured and measured to validate the feasibility of this approach.

1. Introduction

Nowadays, dielectric resonators (DR) can be found in RF/microwave filters for a wide range of industrial applications. Compared with other technologies, DR filters offer a perfect balance between performance and miniaturization. These structures are capable of handling high-power levels while providing a quality factor (Q) comparable to that of pure waveguide implementations [1]. In addition, the overall volume of the component can be significantly reduced thanks to the dielectric properties of the ceramic materials employed. For that reason, DR filters are emerging as the baseline design for many RF filters used in wireless applications [2, 3].

DR filters contain two types of materials: ceramic/dielectric elements (usually in the shape of a post or a puck) that act as resonators, and a metallic enclosure that provides shielding. A recurring issue with this family of filters is how to properly adhere the ceramic parts to the metallic enclosure. For TE configurations, low-permittivity materials are usually glued to the ceramic material and metal walls, properly placing the dielectric resonator within the cavity [4]. However, the manual attachment of these elements frequently leads to misalignment of the parts, resulting in an important degradation of the filter response. At the same time, the use of high-loss adhesive materials to connect the different blocks reduces the performance of the filter in terms of Q factor and insertion losses [5]. In other instances, such as TM dielectric resonator filters, the ceramic block is designed to fit between two parallel walls of the cavity [6]. By doing so, adhesive composites can be eliminated, relying only in the mechanical pressure applied to keep the puck in place (once the cavity is closed). This approach frequently leads to cracks in the ceramic material if the adequate precautions are not taken when assembling the filter. Even in these cases, ensuring a proper contact between the ceramic and metallic parts is not a trivial task.

The importance of developing a simple assembly for DR filters is reflected in the large amount

of publications produced in the last decade that deal with this issue. A large part of the proposed solutions still rely on classical manufacturing techniques for the metallic and ceramic parts [7–10]. However, recent advances in additive manufacturing (AM) techniques have motivated researchers to apply this technology to develop DR with complex shapes to facilitate their assembly within custom-made metallic enclosures [11–14].

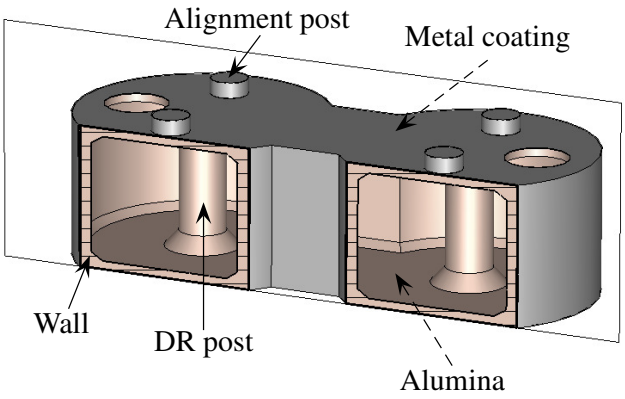

Fig. 1. *View of the proposed two-cavity monoblock ceramic filter.*

The aforementioned solutions involving AM still require the independent manufacture of two parts: the dielectric resonator and the metallic enclosure. In this paper, however, the creation of single-part (i.e. monoblock) TM dielectric resonator filters with AM is proposed as a much simpler and cost-effective alternative to the traditional assembly of DR filters. The body of the filter is fabricated in a single piece of alumina employing the Lithography-based Ceramic Manufacturing (LCM) process, and then coated with a layer of metallic paint (see Fig. 1). By doing so, the proper contact between metal and ceramic surfaces is ensured. Likewise, potential misalignments due to a manual assembly of the filter are minimized, since the resonators are monolithically integrated with the surrounding walls. As depicted, alignment posts are included to facilitate the placement of SMA connectors for the input and output couplings. The proposed configuration takes advantage of the dielectric properties of ceramic materials to decrease the overall volume of the filter, while keeping the structure lightweight, especially compared with monoblock structures completely filled with ceramic material [15–19].

The first part of this paper explains the stereolithography process employed to manufacture the TM dielectric resonator filters. Next, the design and testing of a filter prototype is discussed. Despite the limitations of the proposed filter in terms of geometrical complexity and tunability, this prototype is used to validate the potential application of the AM technology to monoblock ceramic filters. Finally, the main conclusions extracted from this work are summarized.

2. Lithography-based Ceramic Manufacturing

The AM process chosen in this work to develop monoblock ceramic filters is the Lithography-based Ceramic Manufacturing (LCM) technique developed at the Technical University of Vienna and commercialized by Lithoz GmbH [20]. This process is based on layer-by-layer stereolithography that enables the precise manufacturing of complex 3D geometries not suitable for more traditional approaches such as casting and firing.

The complete manufacturing cycle can be split into three steps: manufacturing of the green

body, sample preparation and thermal post-processing.

What differentiates LCM from more traditional manufacturing processes is the way the green body is constructed. Instead of molding or pressing the complete shape of the green body, LCM constructs the body by sequentially stacking layers of a photopolymerizable ceramic suspension. This building material, composed of inorganic ceramic particles and a photoreactive organic binder, is selectively hardened through photopolymerisation when exposed to blue light. A schematic view of the printing process can be found in Fig. 2. When a new layer is to be added to the green body, the building platform is lowered into the vat, submerging the green body in the building material. An optical system, composed of an LED light and a digital micromirror device (DMD) array, transfers the shape of the new layer into the composite via the transparent ground plate of the vat. To do so, the layer of photopolymerizable suspension located between the bottom of the vat and the building platform is selectively hardened in those areas exposed to light. The thickness of this layer can be chosen between 20 and 100 μm. Once the new layer has adhered to the green body, the platform is raised and a wiper blade used to homogeneously refill the vat with the ceramic suspension. The Lithoz CeraFab 7500 system that has been employed in this work has a building envelope of $76 \times 43 \times 150$ mm with a lateral resolution of 40 μm. Other systems are capable of manufacturing larger structures. Depending on the height of the part and the correlating number of layers to print, the process can take a few hours.

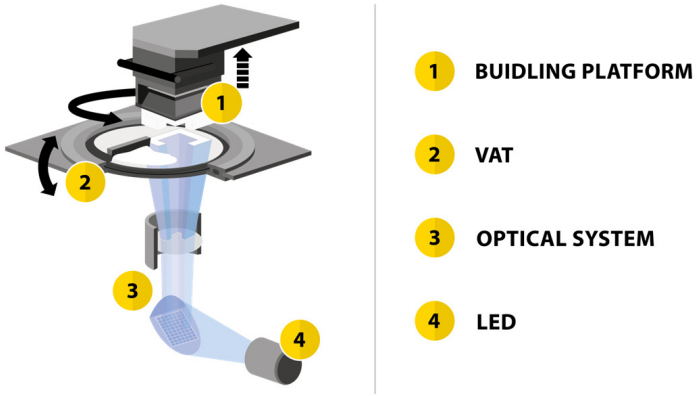

Fig. 2. *System employed to manufacture the green body.*

After the green body is built, it undergoes a process that prepares the sample for the thermal post-processing. In this second step, the structure is manually detached from the building platform. Support structures, frequently employed to ensure the proper orientation of the sample and facilitate the manufacturing of overhangs, are separated from the green body. Then, the excess of uncured material is removed from the structure. An airbrush and a solvent are first employed, followed by the application of an ultrasonic cleaning procedure.

Lastly, two thermal processes are applied to give the material its adequate consistency. First, the sample is introduced in a furnace up to 600°C to remove the polymer binder that keeps the ceramic material together. As it is usually the case when working with ceramic materials, this process (known as thermal debinding) is the most time consuming part of the overall manufacturing procedure. The necessary debinding time depends on the size of the part and the used materials, and is typically between 2 and 7 days. At this stage, it is important to remove the pyrolyzed organic substances from the ceramic part slowly. Otherwise, cracks can be formed in the ceramic part if this process is performed rapidly, due to increasing vapor pressure levels. Finally, the structure is

sintered in a furnace at a temperature that depends on the particular material (1600°C in the case of alumina).

3. Development of a TM dielectric resonator filter compatible with LCM

The goal of this work is to demonstrate the suitability of the LCM process to build monoblock TM dielectric resonator filters made out of alumina ($\varepsilon_r = 9.9$) and externally covered with a metallic paint. A prototype of this filter, the geometry of which can be seen in Fig. 1, is going to be developed to validate this approach. Its main building block is the resonator shown in Fig. 3a, composed of an alumina post, spanning the total height of the resonator, enclosed within walls of the same ceramic material. This block is also surrounded by a thin layer of metallic paint. Before the filter can be constructed, this stand-alone resonator is going to be analyzed.

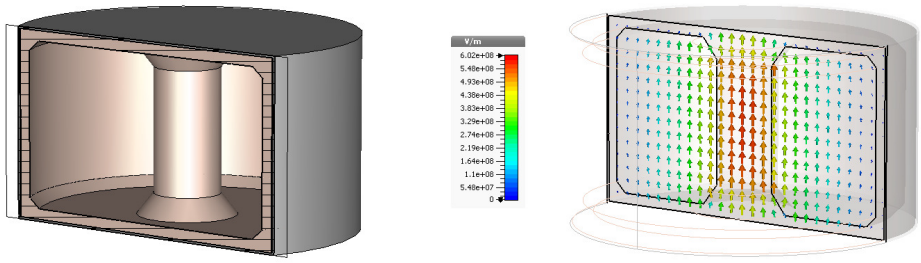

a) b)

Fig. 3. *Single ceramic cavity.*
a) Structure geometry.
b) Electric field distribution at 8.3 GHz.

The fundamental resonance of this structure is the $TM_{01\delta}$ mode of dielectric resonators. As depicted in Fig. 3b, the central post concentrates the electric field within the dielectric material. Consequently, the radius of the lateral wall can be reduced without significantly altering the field distribution or, alternatively, the resonant frequency of the structure (which is mainly controlled by the diameter of the central post). As a result, the structure becomes more compact, roughly 45% smaller than an empty cylindrical cavity resonating at the same frequency.

Traditionally, this type of resonator is built by assembling a cylindrical ceramic rod within a metallic enclosure manufactured by milling. Thanks to AM, nowadays it is possible to manufacture this resonator as a single part. However, in order to use this approach, certain geometrical changes have to be applied: ceramic walls need to be added and interior corners chamfered to avoid thermally-induced stresses during the postprocessing. With the potential to degrade the electrical response of the resonator, it is important to analyze the effects that these changes have on the resonator performance.

3.1. Study of the ceramic wall effect on the resonator performance

The first part of the study involves assessing how the presence and thickness of ceramic walls (instead of metallic ones) affects the spurious-free range (SFR) and the unloaded Q factor (Q_u) of the resonator. On the one hand, the spurious-free range represents the ratio between the frequencies

of the first spurious mode f_{spur} and the fundamental one f_{fund}:

$$\text{SFR} = \frac{f_{\text{spur}}}{f_{\text{fund}}} \tag{1}$$

This magnitude is an indicator of the achievable filter stopband, therefore, the larger this value is, the wider the filter stopband can be. On the other hand, the unloaded Q factor represents the purity of the cavity resonance, and gives an indication of the insertion losses and sharpness of the overall filter response.

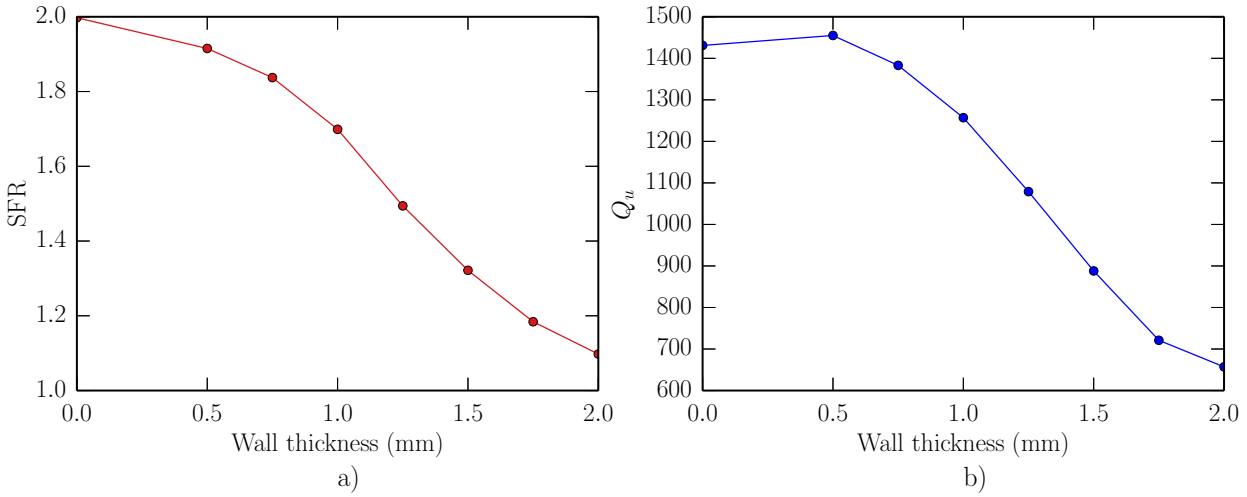

Fig. 4. *Effect of the wall thickness on the resonator performance. Central post radius has been adjusted to ensure that the fundamental mode resonates at* 8.3 *GHz.*
a) Spurious-free range (SFR) as a function of the wall thickness.
b) Unloaded Q factor as a function of the wall thickness.

To ensure a successful manufacture with the LCM process presented in Section 2, walls have to be between 0.5 and 4 mm thick. Thicker walls result in more robust structures, but also heavier. In contrast, thinner walls lead to lighter, yet more fragile, components.

In electrical terms, too much ceramic material on the walls leads to spurious modes resonating at lower frequencies (closer to the fundamental one). This is evidenced by the SFR results depicted in Fig. 4a. If the walls are purely metallic (this is, a wall thickness of 0 mm), the SFR is nearly an octave, but as the ceramic wall becomes thicker, the SFR starts decreasing rapidly.

Another consequence of increasing the wall thickness is that the current density induced on the external metallic walls of the cavity increases. Given that the conductivity of the metallic paint employed is mediocre (around $2.6 \cdot 10^6$ S/m assuming a layer of 25 μm), most of the power lost in the resonator (around 90%) is dissipated by this metallic paint. This fact, combined with the larger volume occupied by dielectric material (thus enhancing dielectric losses), results in larger overall losses as the walls become thicker. Consequently, the Q factor of the resonator decreases as shown in Fig. 4b. In light of these results, the ideal wall thickness for this structure is the minimum achievable, this is 0.5 mm.

3.2. Study of the corner chamfering effect on the resonator performance

Another consequence derived from the use of AM is the need for corner chamfering to minimize mechanical stresses during to the thermal post-processing (especially during sintering, when volume shrinkage takes place). Chamfering corners is only required in the internal walls of the cavity, in particular at the junction between the central post and the horizontal walls, as well as the junction between horizontal and vertical walls.

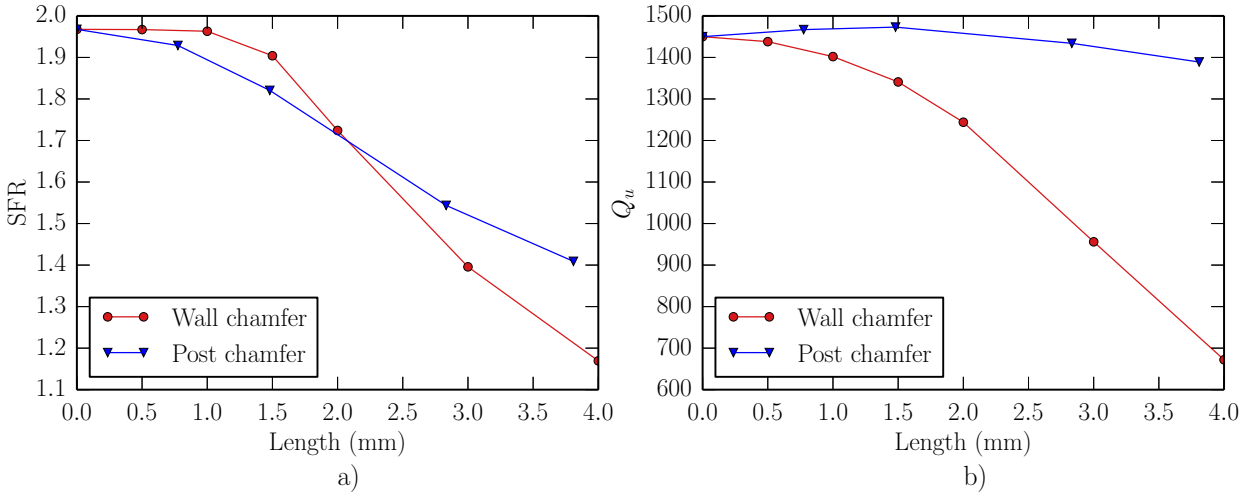

Fig. 5. *Effect of the chamfer length (at the post-wall junctions as well as wall-wall junctions) on the resonator performance. Central post radius has been adjusted to ensure that the fundamental mode resonates at* 8.3 *GHz. Simulations have been performed with a wall thickness of* 0.5 *mm.*
a) Spurious-free range as a function of the chamfer length.
b) Unloaded Q factor as a function of the chamfer length.

In this section, the effect of the corner chamfering on the performance of the stand-alone resonator is studied. Again, the spurious-free range and the unloaded Q factor are computed for multiple values of chamfering length. Results extracted from EM simulations are summarized in Fig. 5. As it is the case for the wall thickness studied in Section 3.1, the results show a very small degradation of the SFR and Q factor for small chamfering lengths (smaller than 1 mm). As the chamfer length becomes larger, higher order modes start to resonate closer to the fundamental one, thus reducing the SFR. Likewise, metal losses increase, especially on the horizontal walls, thus reducing the unloaded Q factor. Therefore, it is important to keep the chamfering length as small as possible.

3.3. Design and measurement of a two-pole filter prototype

After studying the effect that wall thickness and corner chamfering has on the performance of the stand-alone resonator, a two-pole filter prototype is designed. The structure of the filter can be seen in Fig. 1. It is composed of two resonators connected via an inductive iris. The objective response of this filter is centered at 8.3 GHz with a 1.25% fractional bandwidth and return losses better than

17 dB. The coupling matrix representing this response is:

$$M_{\text{obj}} = \begin{bmatrix} 0 & 1.1103 & 0 & 0 \\ 1.1103 & 0 & 1.4212 & 0 \\ 0 & 1.4212 & 0 & 1.1103 \\ 0 & 0 & 1.1103 & 0 \end{bmatrix} \tag{2}$$

From this coupling matrix, the final dimensions of the structure (summarized in Table 1) are derived. In accordance with the study performed in previous sections, the wall thickness and chamfer lengths are set to 0.5 mm. The Q factor of this filter (considering a conductivity of metal paint of $2.6 \cdot 10^6$ S/m) is 1390. A prototype is manufactured in alumina (99.4% T.D.) using the LCM method (see Fig. 6). SMA connectors are then mounted onto the structure to perform measurements.

Table 1 Filter dimensions in mm.

Cavity Radius	Cavity Height	Post Radius	Iris Width	Iris Thickness
7.58	8	1.5	8	4.57

Fig. 6. *Photograph of the manufactured filter prototype.*

Measured results are shown in Fig. 7. As can be seen, the passband of the manufactured filter is shifted 300MHz from the desired frequency. After inspecting a sample that has been manufactured in the same batch without its top cover, it became apparent that the manufactured posts were thicker than designed (the measured diameter was 0.3 mm larger). Since the resonant frequency of the fundamental mode is mainly dependent on the post diameter, this increase can clearly explain the notable frequency shift. As a matter of fact, by simply performing a retro-simulation considering the new post size, it can be seen how the filter passband moves down to 7.95 GHz.

This increase in the post size can be attributed to lateral overpolymerisation during the manufacturing process [21]. Due to the fact that the cavity walls are very thin (only 0.5 mm), the photopolymerizable ceramic suspension requires a high light energy to polymerize the area where walls are located. Since the area of the posts is much larger than that of the walls, there is an excessive exposition of the post cross section to the high light energy, accelerating the photopolymerization process. This results in posts being thicker than desired. A possible solution to this problem would involve increasing the wall thickness in order to reduce the required light energy. However, this solution would also degrade the quality factor and SFR, as demonstrated in previous sections.

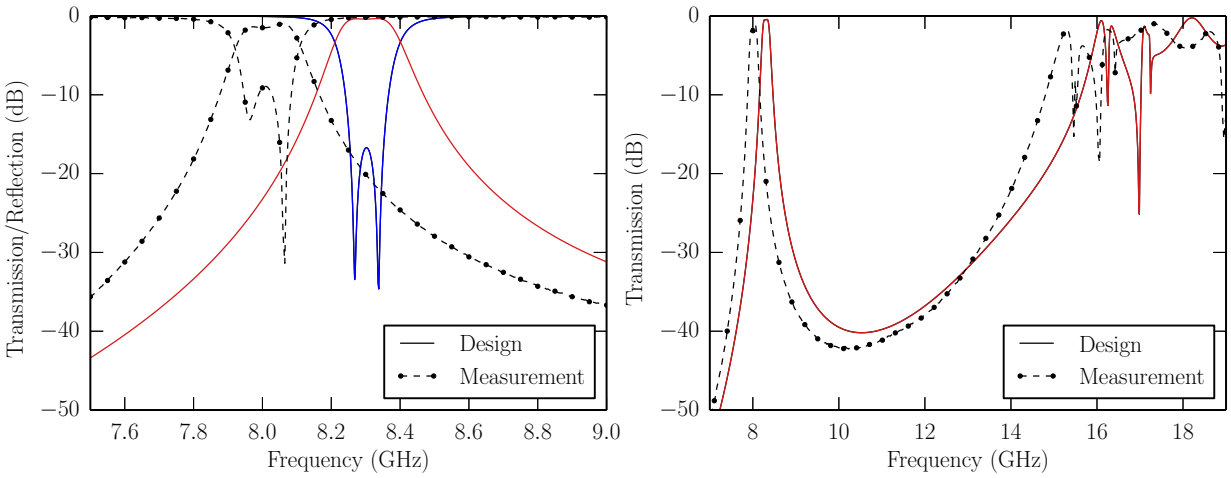

Fig. 7. *Measured response of the filter shown in Fig. 6 compared with design performance.*
a) In-band response.
b) Wideband response depicting the spurious resonances.

From the measured response, we can also extract an approximate value for the effective conductivity of the metallic paint, including the effect of the surface roughness. Within the passband, the measured insertion losses are 1.5 dB (0.6 dB are due to the poor matching, and the rest to losses). After performing a parameter extraction, the estimated conductivity is around $\sigma \approx 4 \cdot 10^5$ S/m, a significantly lower value than originally expected. Inserting this material in the EM simulations, it can be concluded that the Q factor of these resonators is around 600. As far as the spurious-free range is concerned, it can be clearly seen in Fig. 7b that the first spurious mode resonates at approximately 15.3 GHz, resulting in an effective SFR of 1.91 (consistent with the original design). In summary, these results prove that LCM is a suitable technology to develop monoblock ceramic filters, although significant additional work is needed for this technology to compete with the existing classical manufacturing approaches for DR filters.

4. Conclusions

This paper has proposed the use of AM to overcome some of the problems associated with the assembly of TM dielectric resonator filters. This technology enables the creation of monoblock ceramic structures that integrate the dielectric resonator (post) with the surrounding walls and alignment posts, to facilitate the assembly of SMA connectors. For shielding purposes, a metallic paint is applied on the outside of the structure, ensuring proper contact at the ceramic-metal interface. The result is a compact structure that requires almost no assembly (mainly the placement of connectors).

The lithography-based ceramic manufacturing process has been employed to develop these filters. A brief overview of this approach has been presented in Section 2. The choice of this technology to manufacture filters implies certain geometrical changes compared with classical implementations. A study has been included to assess how the presence of chamfered corners, as well as ceramic walls (in addition to metallic ones), affects the spurious-free range and unloaded Q factor of resonators manufactured with this technique. Finally, a two-pole filter prototype has been

manufactured and measured to demonstrate the feasibility of this approach to successfully develop TM dielectric resonator filters. Although there were some discrepancies between measured and simulated results, it has been possible to extract valuable conclusions that will help improve the manufacturing process for future development of dielectric resonator filters.

5. Acknowledgments

This work was supported by the Austrian Research Promotion Agency FFG under R&D project No. 854026. The authors would like to thank Mr. Sebastian Sattler, Technische Universität Graz, for his assistance in the assembly and measurement of the filter prototype.

6. References

[1] R. Cameron, C. Kudsia, and R. R. Mansour, *Microwave filters for communication systems*. Hoboken, N.J.: Wiley-Interscience, 2007.

[2] R. R. Mansour, "Filter technologies for wireless base stations," *IEEE Microw. Mag.*, vol. 5, no. 1, pp. 68–74, Mar. 2004.

[3] A. Knack, J. Mazierska, and H. Piel, "Dielectric Resonator Filters for UMTS Systems," in *IEEE MTT-S International Microwave Workshop Series on Art of Miniaturizing RF and Microwave Passive Components*, Dec. 2008, pp. 30–33.

[4] S. Bastioli and R. V. Snyder, "In-line pseudoelliptic TE01d mode dielectric resonator filters," in *IEEE MTT-S Int. Microwave Symp. Dig.*, June 2012, pp. 1–3.

[5] R. R. Mansour, "High-Q tunable dielectric resonator filters," *IEEE Microw. Mag.*, vol. 10, no. 6, pp. 84–98, Oct. 2009.

[6] L. Pelliccia, F. Cacciamani, C. Tomassoni *et al.*, "Ultra-compact filters using TM dual-mode dielectric-loaded cavities with asymmetric transmission zeros," in *IEEE MTT-S Int. Microwave Symp. Dig.*, June 2012, pp. 1–3.

[7] A. Panariello, M. Yu, and C. Ernst, "Ku-Band High Power Dielectric Resonator Filters," *IEEE Trans. Microw. Theory Tech.*, vol. 61, no. 1, pp. 382–392, Jan. 2013.

[8] X. Wang and K. L. Wu, "A TM_{01} Mode Monoblock Dielectric Filter," *IEEE Trans. Microw. Theory Tech.*, vol. 62, no. 2, pp. 275–281, Feb. 2014.

[9] R. Zhang and R. R. Mansour, "Low-Cost Dielectric-Resonator Filters With Improved Spurious Performance," *IEEE Trans. Microw. Theory Tech.*, vol. 55, no. 10, pp. 2168–2175, Oct 2007.

[10] ——, "Dielectric Resonator Filters Fabricated from High-K Ceramic Substrates," in *IEEE MTT-S Int. Microwave Symp. Dig.*, June 2006, pp. 234–237.

[11] N. Delhote, D. Baillargeat, S. Verdeyme *et al.*, "Narrow Ka Bandpass Filters Made Of High Permittivity Ceramic By Layer-By-Layer Polymer Stereolithography," in *European Microwave Conference (EuMC)*, Sept 2006, pp. 510–513.

[12] ——, "Innovative Shielded High Q Dielectric Resonator Made of Alumina by Layer-by-Layer Stereolithography," *IEEE Microw. Wireless Compon. Lett.*, vol. 17, no. 6, pp. 433–435, June 2007.

[13] L. Carpentier, N. Delhote, S. Verdeyme *et al.*, "Compact Ku band filter based on BMT dielectric resonators made in a single part using 3D ceramic stereolithography process," in *IEEE MTT-S Int. Microwave Symp. Dig.*, June 2012, pp. 1–3.

[14] Y. Marchives, N. Delhote, S. Verdeyme *et al.*, "Wide-band dielectric filter at C-band manufactured by stereolithography," in *European Microwave Conference (EuMC)*, Oct. 2014, pp. 187–190.

[15] A. H. Khalil, N. Delhote, S. Pacchini *et al.*, "3-D pyramidal and collective Ku band pass filters made in Alumina by ceramic stereolithography," in *IEEE MTT-S Int. Microwave Symp. Dig.*, June 2011, pp. 1–4.

[16] F. Kouki, M. Thevenot, S. Bila *et al.*, "Miniature ceramic filter-antenna for wireless communications systems at 60 GHz," in *European Microwave Conference (EuMC)*, Oct. 2014, pp. 1588–1591.

[17] I. C. Hunter and M. Y. Sandhu, "Monolithic integrated ceramic waveguide filters," in *IEEE MTT-S Int. Microwave Symp. Dig.*, June 2014, pp. 1–3.

[18] Y. Jang, J. Kim, S. Kim *et al.*, "Design and Fabrication of a Compact 3-Dimensional Stacked Type Dielectric Ceramic Waveguide Bandpass Filter," *IEEE Microw. Wireless Compon. Lett.*, vol. 24, no. 10, pp. 665–667, Oct. 2014.

[19] I. Hunter, S. Afridi, and M. Sandhu, "Integrated ceramic waveguide filters with improved spurious performance," in *European Microwave Conference (EuMC)*, Sept. 2015, pp. 674–677.

[20] U. K. Fischer, N. Moszner, V. Rheinberger *et al.*, *Light-curing ceramic slips for the stereolithographic preparation of high-strength ceramics*. U.S. Patent: 9403726 B2, Mar. 2014.

[21] S. Gentry and J. Halloran, "Depth and width of cured lines in photopolymerizable ceramic suspensions," *Journal of the European Ceramic Society*, vol. 33, no. 10, pp. 1981–1988, Mar. 2013.